Angle Dependent Collective Surface Plasmon Resonance in an Array of Silver Nanoparticles†

Anatoliy O. Pinchuk

Department of Physics and Energy Sciences, University of Colorado at Colorado Springs, 1420 Austin Bluffs Pkwy, Colorado Springs, Colorado 80933

Received: December 15, 2008; Revised Manuscript Received: February 27, 2009

Theoretical analysis of the scattering efficiency of an equidistantly spaced regular array of spherical silver nanoparticles reveals a nonmonotonic shift of the collective SPR wavelength and its bandwidth depending on the distance between the particles and the angle of the incidence of the linear polarized electromagnetic wave. The far-field electromagnetic coupling between the particles in the chain exhibits the largest range of angular tuning of the collective SPR band when the distance between the particles in the chain approaches that of the collective SPR wavelength. The dependence of the SPR wavelength and its bandwidth on the angle of the incidence of the linear polarized electromagnetic wave and the distance between the particles in the chain provides an additional flexibility for the development of optical biochemical sensors and subwavelength waveguides.

1. Introduction

Collective coherent electronic excitations in noble metal nanostructures known as surface plasmon resonance[1,2] (SPR) have recently shaped a new field of research called plasmonics.[3−5] A lot of experimental and theoretical efforts have been devoted to plasmonic nanostructures[3,6−8] due to their unique optical and electronic properties, which can be used in such diverse applications as surface enhanced spectroscopy,[9,10] e.g., surface enhanced Raman spectroscopy[11−15] (SERS), surface enhanced fluorescence,[16] surface enhanced near-infrared (NIR) spectroscopy,[10] novel ultrasensitive optical biochemical sensors,[17−20] optical waveguides,[20−22] plasmon-emitting diodes,[23] and plasmonic transistors, to name just a few. Metal nanoshells have been studied for biochemical and medical applications, such as cancer treatment.[24]

Electromagnetic coupling between metal nanoparticles is of much interest for the development of optical subwavelength waveguides.[6,25−31] Light channeling along coupled nanoparticle waveguides would allow one to integrate optical and electronic circuits on the nanoscale.[32] Direct experimental observation of the near-field coupling and transfer of electromagnetic energy between closely spaced nanoparticles and nanorods conceptually proved this idea.[33,34] In a recent experiment, gold nanoparticle chains were fabricated using electron-beam lithography (EBL) following chemical etching and a lift-off process.[35] Nanoparticles were cylindrical in shape, with 9 nm height and around 90 nm diameter. The near field optical patterns were collected using photon scanning tunneling microscope (PSTM) in the scattering mode. The far-field radiative coupling between the particles in the chain was studied for the distances between the particles large compared to their size. The samples were optically excited by the near field in the total internal reflection mode.[35] The nonuniform shift of the SPR collective mode was observed in the system of coupled nanoparticles and the transfer of electromagnetic energy along the chain was confirmed. Optical coupling between noble metal nanoparticles can be employed for the development of biochemical sensors.[20,36−41] Tuning the collective SPR mode in such structures can be achieved by varying the distance between the particles.[37,42−46] The coupling between molecular resonance of target molecules and the SPR collective mode can then be used for the development of ultrasensitive optical biochemical sensors.[17,18,44] Propagating surface plasmon polariton modes at the metal−dielectric interface is an alternative approach to the development of biochemical sensors.[47] Target molecules functionalized on the metal−dielectric interface change the local index of refraction, which leads to the shift of the minimum in the reflected light beam caused by the resonant excitation of the propagating SPR mode.[48] This principle can be extended to the wavelength and angle dependent SPR spectroscopy and ultimately be used in multicolor SPR optical spectroscopy with enhanced sensitivity.[47]

Local field enhancement and tuning of the collective SPR in a chain of gold nanoparticles was also studied theoretically with the assumption of an evanescent excitation through total internal reflection.[49] The SPR wavelength and width of the collective SPR mode was shown to be dependent on the excitation conditions such as the polarization of the incident light, interparticle distance and the angle of the incidence of the excitation electromagnetic wave. A string-type collective SPR mode was suggested as a possible coupling mechanism, which generates large electromagnetic field enhancement close to the particles constituting the chain.[49]

In a recent paper, we studied a chain of spherical silver nanoparticles embedded in a glass host medium.[50] The collective SPR mode of the chain was shown to strongly depend on the distance between the particles.[50] When the distance between the particles in the array approaches to that of the wavelength of the collective SPR mode of the chain, the SPR scattering efficiency is enhanced and the bandwidth narrowes.[50]

Most of the theoretical and experimental efforts so far have been focused on the near- and far-field electromagnetic coupling between nanoparticles as a function of the distance between the particles.[35,37,42,43,50,51] The near-field coupling between closely spaced nanoparticles leads to a strong shift of the coupled SPR band[52,53] and to additional quadrupolar and higher-order multipoles peaks[54] in the extinction spectra.[55] The shift of the

† Part of the "George C. Schatz Festschrift".

10.1021/jp811067r CCC: $40.75
Published on Web 03/13/2009

collective SPR band depends on the polarization of the incident light.[50,55] When nanoparticles overlap and form elongated structures, their optical response is influenced by the conductive coupled regime and resembles those of spheroidal particles.[56] However, the dependence of the collective SPR band in a chain of spherical nanoparticles on the angle of the incidence of electromagnetic wave and simultaneously on distance between the particles has not been addressed. Such study would be of interest for the development of optical waveguides and biochemical sensors. Tuning the SPR band by changing the angle of the incidence of the excitation light and the distance between the particles would add an additional degree of freedom and flexibility to the development of plasmonic biochemical sensors and optical waveguides.

In this paper, we address theoretically the coupling of the collective SPR mode depending on the angle of the incidence of the incoming light and the distance between the particles in the chain. We use the generalized Mie theory to examine the behavior of the collective SPR band in a system of spherical nanoparticles equidistantly arranged in the chain as a function of the distance between the particles in the chain and the angle of the incidence of an electromagnetic wave. The theory proved to be one of the most rigorous theoretical methods for describing optical response of coupled nanoparticles.

In section 2, we outline the generalized Mie theory of scattering of electromagnetic waves by an arbitrary system of spherical nanoparticles. In section 3, we describe the numerical results of the collective SPR mode in a system of optically coupled nanoparticles and the influence of the distance between the particles and the angle of the incidence of the incoming light, following the discussion and conclusions.

2. Generalized Mie Theory

The theory of light scattering by a spherical particle was developed by Gustav Mie and independently by Peter Debye a hundred years ago.[2] Commonly known as the Mie theory, it is based on the expansion of the incident, internal, and scattered electromagnetic waves into vector spherical harmonics and the standard boundary conditions to match the fields at the interface between the sphere and embedding host medium.[2] The theory has been successfully used for calculations of the optical response of a single sphere and collections of noninteracting spherical particles.[1,2] An extended Mie theory exists for some other regular shapes of nanoparticles, such as ellipsoids and cylinders, for which there are available analytical expressions for the expansion of the electromagnetic fields into corresponding vector harmonics.[1,2] The grid methods, such as discrete dipole approximation (DDA)[57] or finite-difference time-domain (FDTD),[58,59] have been developed for nonspherical nanoparticles, including cubes, triangles, and hexagons. The T-matrix method is an alternative exact theory for calculation of the extinction of light by coupled nanoparticles.[60−62] The T-matrix and the generalized Mie theory are equivalent theoretical methods for regular particles, e.g., spheres or ellipsoids, but the advantage of the T-matrix is that it can also be used for irregular nanoparticles such as cubes, triangles, etc.[61] Because our problem includes arrays of regular spherical nanoparticles, we will use the generalized Mie theory.[63]

Scattering of light by a system of closely spaced nanoparticles leads to electromagnetic coupling between the particles, which can significantly modify the extinction spectra of the system. The theory of light scattering by a system of electromagnetically coupled spheres was developed by Gerardy and Ausloos,[63,64] who applied the approach of the generic Mie theory to take into account the scattered electromagnetic field from neighbor nanoparticles. The theory takes into account both retardation and multipole effects.

In this section, we briefly outline the theory and give an expression for the scattering cross section of a system of spherical nanoparticles,[63,64] which is used in the next section to calculate the scattering by a chain of spherical silver nanoparticles. The expansion of the incident $\mathbf{E}_0$, scattered $\mathbf{E}_s = \sum_{i=1}^{N_s} \mathbf{E}_s^i$ and internal $\mathbf{E}_1$ electromagnetic fields into vector spherical harmonics are given by[65]

$$\mathbf{E}_0 = \sum_{n=1}^{\infty} \sum_{m=-n}^{n} (p_{nm}\mathbf{N}_{nm}^{(1)}(r,\theta,\phi) + q_{nm}\mathbf{M}_{nm}^{(1)}(r,\theta,\phi)) \quad (1)$$

$$\mathbf{E}_s^i = \sum_{i=1}^{N_s} \sum_{n=1}^{\infty} \sum_{m=-n}^{n} (a_{mn}^i \mathbf{N}_{nm}^{(3)}(r^i,\theta^i,\phi^i) + b_{mn}^i \mathbf{M}_{nm}^{(3)}(r^i,\theta^i,\phi^i)) \quad (2)$$

$$\mathbf{E}_1^i = \sum_{n=1}^{\infty} \sum_{m=-n}^{n} (d_{mn}^i \mathbf{N}_{mn}^{(1)}(r^i,\theta^i,\phi^i) + c_{mn}^i \mathbf{M}_{nm}^{(1)}(r^i,\theta^i,\phi^i)) \quad (3)$$

where the vector spherical harmonics are given by[66] $M_{nm}^{(j)} = \nabla \times r u_{nm}^{(j)}$ and $N_{nm}^{(j)} = (1/k)\nabla \times M_{nm}^{(j)}$. The scalar spherical harmonics $u_{nm}^{(j)}$ are related to the spherical Bessel functions of the first, j_n, and second kind,[67] $h_n = j_n + iy_n$ through $u_{nm}^{(1)} = j_n(r)\, p_n^m(\cos\theta)e^{im\phi}$ and $u_{nm}^{(3)} = h_n(r)\, p_n^m(\cos\theta)e^{im\phi}$, where $P_n^m(\cos\theta)$ stands for the associated Legendre functions. The superscripts (1) and (3) in eqs 1−3 refer to the first and the third kind of the scalar spherical harmonics used in the expansion of the vector spherical harmonics. The choice of the corresponding scalar spherical harmonics is dictated by the requirement of regular behavior of the electric fields at infinity and the origin of the coordinate system. The unknown coefficients a_{nm}^i, b_{nm}^i, c_{nm}^i, d_{nm}^i of the expansions are found by applying standard boundary conditions at the surface of a chosen nanoparticle: $(\mathbf{E}_0 + \mathbf{E}_s - \mathbf{E}_1) \times \hat{e}_r = 0$ and $(\mathbf{H}_0 + \mathbf{H}_s - \mathbf{H}_1) \times \hat{e}_r = 0$. This can be done by using the addition theorem for the vector spherical harmonics, which transforms the expansion series of the vector spherical harmonics around each NP of the cluster to the chosen NP and, thus, allows one to match the boundary conditions in the same, spherical coordinate system.[65] After matching the standard boundary conditions, the coefficients of expansion a_{nm}^i and b_{nm}^i can be found from a linear set of coupled equations

$$a_{nm}^i = -\alpha_n^i \Big(p_{nm}^i + \sum_{j=1,j\neq 1}^{N} \sum_{l=1}^{\infty} \sum_{k=-l}^{l} A_{nm}^{kl}(r^{ij},\Theta^{ij},\phi^{ij}) a_{kl}^i + B_{nm}^{kl}(r^{ij},\Theta^{ij},\phi^{ij}) b_{kl}^j\Big)$$

$$b_{nm}^i = -\beta_n^i \Big(q_{nm}^i + \sum_{j=1,j\neq 1}^{N} \sum_{l=1}^{\infty} \sum_{k=-l}^{l} A_{nm}^{kl}(r^{ij},\Theta^{ij},\phi^{ij}) b_{kl}^j + B_{nm}^{kl}(r^{ij},\Theta^{ij},\phi^{ij}) a_{kl}^j\Big) \quad (4)$$

where α_{nm}^i and β_{nm}^i are the usual Mie coefficients[1]

$$\alpha_n^i = \frac{m^i\psi_n'(x^i)\,\psi_n(m^ix^i) - \psi_n(x^i)\,\psi_n'(m^ix^i)}{m^i\xi_n'(x^i)\,\psi_n(m^ix^i) - \xi_n(x^i)\,\psi_n'(m^ix^i)}$$
$$\beta_n^i = \frac{\psi_n'(x^i)\,\psi_n(m^ix^i) - m^i\psi_n(x^i)\,\psi_n'(m^ix^i)}{\xi_n'(x^i)\,\psi_n(m^ix^i) - m^i\xi_n(x^i)\,\psi_n'(m^ix^i)} \quad (5)$$

where m^i is the refractive index of the metal NP relative to the refractive index of the host medium, m_h, $x^i = kR_i$ is a dimensionless parameter, R_i is the radius of NPs, $k = 2\pi/\lambda$, where λ is the wavelength, and ψ, ψ' and ζ, ζ' are respectively the Riccati−Bessel functions and their derivatives. The extinction cross section of a system of nanoparticles arbitrarily arranged in space is given by

$$Q_{ext} = \frac{2\pi}{k^2}\sum_{i=1}^{N}\sum_{n=1}^{\infty}\sum_{m=-n}^{n}\frac{n(n+1)(n+m)!}{(2n+1)(n-m)!}\mathrm{Re}[a_{nm}^i p_{nm}^{*i} + b_{nm}^i q_{nm}^{*i}] \quad (6)$$

where N is the number of the nanoparticles in the system. The scattering efficiency is given by

$$Q_{scat} = \frac{2\pi}{k^2}\sum_{i=1}^{N}\sum_{n=1}^{\infty}\sum_{m=-n}^{n}\frac{n(n+1)(n+m)!}{(2n+1)(n-m)!}(|a_{nm}^i|^2 + |b_{nm}^i|^2) \quad (7)$$

The absorption efficiency can be calculated as using the scattering and extinction efficiencies $Q_{ext} = Q_{abs} + Q_{scat}$.

3. Numerical Results and Discussion

In this section, we use the aforementioned theory to examine the behavior of the collective SPR in a chain of metal spherical nanoparticles as a function of the distance between the particles and the angle of the incidence of the linear polarized electromagnetic wave. As a model system, we consider $N = 10$ spherical silver nanoparticles of same radius $R = 25$ nm equidistantly arranged in a chain with the distance between the centers of the particles d; see Figure 1. The choice of the geometry (the size and spacing between the particles) is dictated by the current state-of-the-art development of electron-beam and ion-beam lithographic techniques. The size of the particles was chosen to enable effective coupling between the particles through the scattering of the incident electromagnetic wave. The nanoparticles are embedded in an isotropic transparent host medium with a refractive index $n = 1.51$ (glass). We change the angle of the incidence of the linear polarized electromagnetic wave in small increments ($\Delta\theta = 10°$) from the normal $\theta = 0°$ and up to the grazing incidence angle $\theta = 90°$. The incident electromagnetic wave is linear polarized either in the plane of the incidence (p polarization) or perpendicular to this plane (s polarization), as depicted in Figure 1. The frequency dependent complex dielectric permittivity for silver was taken from the literature.[68] We calculated the scattering efficiency (normalized scattering cross section) of the chain as a function of the angle of the incidence θ and the wavelength of the incoming light λ. Specifically, we are interested in the far-field radiative electromagnetic coupling between the particles in the chain. Our calculations indicate that the scattering efficiency spectra are not affected when the multipolar order increases higher than $l = 3$, so we restrict our analysis to this multipolar order. Scattering of the incoming electromagnetic wave leads

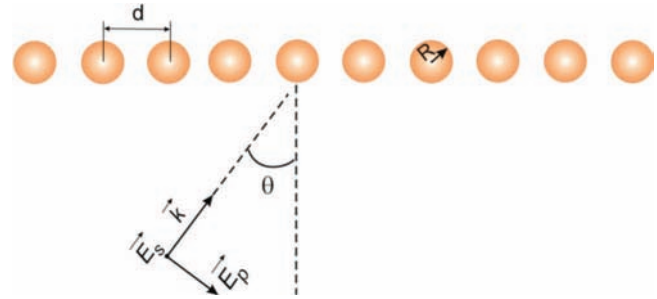

Figure 1. Chain of spherical nanoparticles illuminated by a linear polarized electromagnetic wave with two mutually perpendicular polarizations $\boldsymbol{E}_s$ and $\boldsymbol{E}_p$.

to electromagnetic coupling between the particles in the chain and causes the excitation of a collective SPR mode of the chain, whose wavelength and bandwidth depends on the distance between the particles. The near field coupling prevails the scattering spectra when the distance between the particles in the chain varies in the range 2−4 radii of the particles (50−200 nm in our case);[50] therefore, we begin our calculations with the distance between the particles ($d = 200$ nm), where the far-field radiative coupling prevails the scattering spectra. The far-field radiative coupling between regular spaced two-dimensional nanoparticle arrays[69] and one-dimensional chains[70] leads to a significant shift of the collective SPR band and its broadening. In addition, strong local electric field enhancement might be used to enhance the fluorescence efficiency of molecules functionalized on the surface of nanoparticles.[71]

Let us first consider the chain when the distance between the particles is $d = 200$ nm, Figure 2. The scattering efficiency spectra for s and p linear polarized electromagnetic wave are shown in Figure 2a,b. Dashed line represents the scattering efficiency of a single $R = 25$ nm silver nanoparticle, when no coupling is present in the system. We skipped a few angles of the incidence for the sake of clarity of the plot. A change in the angle of the incidence of the electromagnetic wave causes a nonmonotonic shift and broadening of the collective SPR band, Figure 2a,b.

The collective SPR wavelength is approximately the same for both s and p polarization of the incident wave at normal incidence ($\theta = 0°$), $\lambda_{SPR} \approx 425$ nm, as shown in Figure 2c. Initially, the increase of the angle of the incidence leads to a red shift of the collective SPR wavelength for both s and p polarization of the incident light. The red shift for the s-polarized electromagnetic wave is $\Delta\lambda_{SPR} = 13$ nm (from λ_{SPR} 425 nm to $\lambda_{SPR} = 438$ nm) and $\Delta\lambda_{SPR} = 10$ nm (from λ_{SPR} 425 nm to $\lambda_{SPR} = 435$ nm) for the p-polarized electromagnetic wave, Figure 2c. An increase of the angle of the incidence larger than $\theta = 25°$ leads to a blue shift which follows the red one for both s and p polarization of the incident light. This shifts the collective SPR wavelength to $\lambda_{SPR} = 428$ nm at the incident angle $\theta = 45°$ for the s-polarized electromagnetic wave and to $\lambda_{SPR} = 431$ nm at the incident angle $\theta = 60°$ for the p-polarized electromagnetic wave. Further increase of the angle of the incidence leads to a red shift for both s- and p-polarized electromagnetic waves which results in $\lambda_{SPR} = 435$ nm for both polarizations of the incoming light. There are fives angles of the incidence of the incoming light where the wavelength of the collective SPR is the same for both polarizations of the incoming light, that is, when the chain becomes isotropic with respect to the linear polarized electromagnetic wave: $\theta = 9°$, $\lambda_{SPR} = 426$ nm; $\theta = 17°$, $\lambda_{SPR} = 428$ nm; $\theta = 35°$, $\lambda_{SPR} = 435$ nm; $\theta = 66°$, $\lambda_{SPR} = 423$ nm; $\theta = 90°$, $\lambda_{SPR} = 435$ nm. The maximum range of tuning

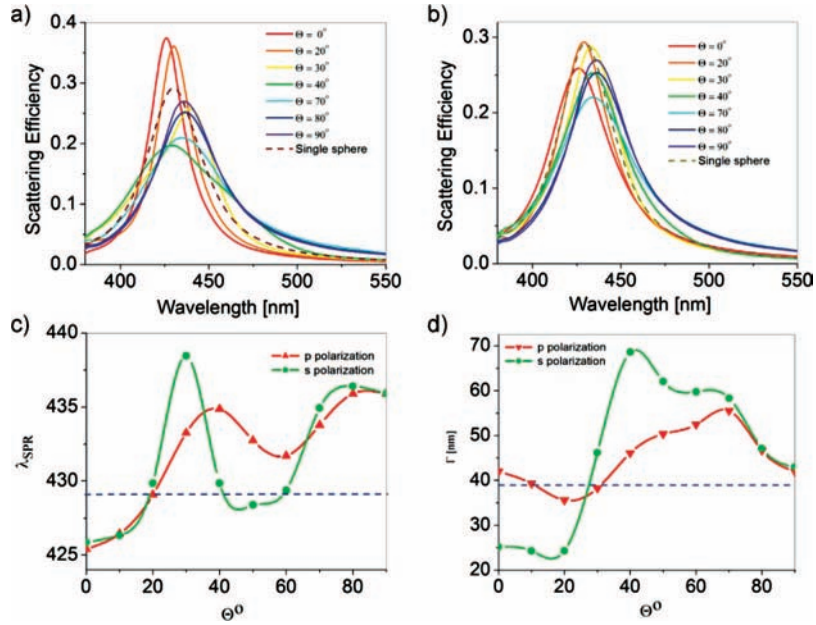

Figure 2. Scattering of a linear polarized electromagnetic wave by a chain of spherical silver nanoparticles. The distance between the particles in the chain is $d = 200$ nm. The dashed line represents the scattering efficiency of a single spherical nanoparticle. (a) Scattering efficiency (normalized scattering cross section) for s-polarized electromagnetic wave as a function of the wavelength and the angle of the incidence θ. (b) Scattering efficiency for p-polarized electromagnetic wave. (c) Collective SPR wavelength λ_{SPR} as a function of the incident angle for s- and p-polarized electromagnetic fields. (d) Bandwidth of the collective SPR as a function of the incident angle for s- and p-polarized electromagnetic fields.

of the SPR wavelength is $\Delta\lambda_{SPR} = 13$ nm for s polarization and $\Delta\lambda_{SPR} = 9$ nm for p polarization of the incident electromagnetic wave.

Figure 2d shows the bandwidth of the collective SPR of the chain as a function of the angle of the incidence. At normal incidence ($\theta = 0°$), the bandwidth Γ of the SPR differs for s and p polarization $\Gamma_s = 25$ nm and $\Gamma_p = 42$ nm. Increase of the angle of the incidence narrows the SPR band for both s and p polarizations of the incident light as shown in Figure 2b. The increase of the angle of the incidence larger than $\theta = 20°$ broadens the collective SPR band for both polarizations. The broadening extends to $\Gamma = 69$ nm at $\theta = 41°$ for s polarization of the incident light and to $\Gamma = 56$ nm at $\theta = 68°$ for p polarization of the incident light. At the angle of the incidence $\theta = 27°$ both s and p polarization have the same bandwidth. At the grazing angle $\theta = 90°$ both p polarization and s polarization of the incident light have the same bandwidth $\Gamma = 42$ nm. The maximum range of change of the width of collective SPR resonance is $\Delta\Gamma_s = 47.5$ nm and $\Delta\Gamma_p = 20$ nm. The minimum bandwidth $\Gamma_s = 23$ nm is observed at $\theta = 16°$.

The analysis of the far-field radiative coupling between regularly arranged nanoparticle arrays using Hertz-vector representations indicates two different coupling regimes between the particles: radiative plane waves and evanescent coupling.[72,73] The transition between radiative and evanescent coupling occurs when the in-plane wave vector of the incident electromagnetic wave crosses the light circle $|\mathbf{k}_{||}| = k$ in the Fourier-series representation.[72] This marks different grating orders within the lattice array. When the coupling becomes radiative, the damping increases, which leads to an increase of the bandwidth of the collective SPR mode.[72] The evanescent coupling red-shifts the SPR band, and the transition to the radiative coupling blue-shifts the collective SPR wavelength.[73] Thus, the nonmonotonic shift and broadening of the SPR band in the array of silver nanoparticles is caused by different coupling regimes between the particles.[74,75] Once the collective SPR mode becomes evanescent, its wavelength undergoes a red shift. The shift in the opposite direction occurs when the collective SPR mode switches to radiative coupling. The transition from radiative to evanescent nature of the collective SPR mode can be interpreted as the change of the grating order of the chain.[74] This effect should be observed in two-dimensional arrays of nanoparticles, but the quantitative shift and broadening should be of different magnitude.[69] A nonmonotonic shift of the SPR band was noticed, though as a minor effect in a recent theoretical publication.[60] The shift was small because the authors did not reach the first grating order where the particles interact strongly.[60]

Let us increase the distance between the particles up to $d = 250$ nm and consider the evolution of the scattering efficiency of the chain as a function of the angle of incidence of the electromagnetic wave, Figure 3a,b. The dependence of the scattering efficiency on the angle of the incidence reveals itself slightly different from the case $d = 200$ nm, Figure 2a,b. The SPR wavelength is different for s polarization ($\lambda_{SPR} = 432$ nm) and for p polarization ($\lambda_{SPR} = 427$ nm) at the normal incidence $\theta = 0°$, Figure 3e. When the angle of the incidence increases, we observe a red shift for both s and p polarization of the incident light, Figure 3c. At the angle $\theta = 17°$, we observe an isotropic response of the system; that is, both s and p polarizations have the same SPR wavelength $\lambda_{SPR} = 430$ nm. Following the red shift, the SPR band blue-shifts at the angle of the incidence $\theta = 10°$ for s-polarized electromagnetic wave and at $\theta = 25°$ for p-polarized electromagnetic wave. The SPR wavelength reverses the shift to the red part of the spectrum at the angle $\theta = 30°$ for s-polarized and at $\theta = 40°$ for the p-polarized electromagnetic wave, Figure 3c. The maximum range of tuning of the SPR wavelength is $\Delta\lambda_{SPR} = 12$ nm for s polarization and $\Delta\lambda_{SPR} = 10$ nm for p polarization, which is very close to the previous case, $d = 200$ nm.

The angle dependent SPR bandwidth exhibits a similar evolution as in the case of $d = 200$ nm; compare Figure 3d and Figure 2d. The maximum range of the change of the width of the collective SPR band is $\Delta\Gamma_s = 30$ nm and $\Delta\Gamma_p = 15$ nm,

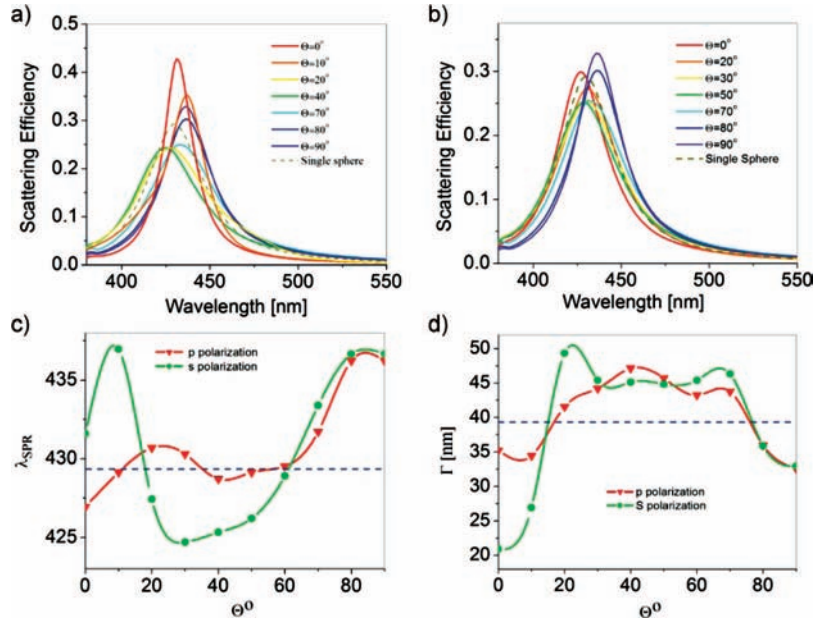

Figure 3. Scattering of a linear polarized electromagnetic wave by a chain of spherical silver nanoparticles. The distance between the particles in the chain is $d = 250$ nm. The dashed line represents the scattering efficiency of a single spherical nanoparticle. (a) Scattering efficiency (normalized scattering cross section) for s-polarized electromagnetic wave as a function of the wavelength and the angle of the incidence θ. (b) Scattering efficiency for p-polarized electromagnetic wave. (c) Collective SPR wavelength λ_{SPR} as a function of the incident angle for s- and p-polarized electromagnetic fields. (d) Bandwidth of the collective SPR as a function of the incident angle for s- and p-polarized electromagnetic fields.

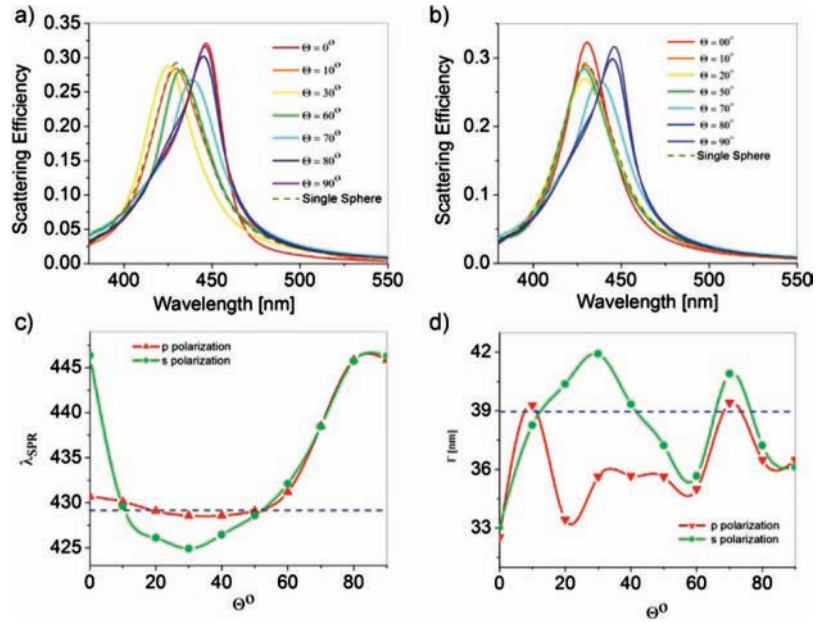

Figure 4. Scattering of a linear polarized electromagnetic wave by a chain of spherical silver nanoparticles. The distance between the particles in the chain is $d = 300$ nm. The dashed line represents the scattering efficiency of a single spherical nanoparticle. (a) Scattering efficiency (normalized scattering cross section) for s-polarized electromagnetic wave as a function of the wavelength and the angle of the incidence θ. (b) Scattering efficiency for p-polarized electromagnetic wave. (c) Collective SPR wavelength λ_{SPR} as a function of the incident angle for s- and p-polarized electromagnetic fields. (d) Bandwidth of the collective SPR as a function of the incident angle for s- and p-polarized electromagnetic fields.

which is significantly lower than for the distance d-200 nm. The minimum bandwidth $\Gamma_s = 21$ nm is observed at normal incidence $\theta = 0°$.

The nonmonotonic shift of the collective SPR band in a chain of noble metal nanoparticles coupled through far-field radiation was observed experimentally[52,69,76] and theoretically[77] as a function of the distance between the particles in the chain and the polarization of the incident light.[42] The nonmonotonic shift of the collective SPR band was rationalized by different strength of the coupling dipole for mutually orthogonal polarizations of the excitation light[78,79] and different gating orders which result from evanescent and radiative coupling between the particles in the chain.[75] In addition, the nonmonotonic shift of the coupled SPR band was observed for varying number of the particles in a chain.[70]

Finally, let us consider the distance between the particles in the chain $d = 300$ nm, Figure 4a,b. At normal incidence $\theta = 0°$, we observe the collective SPR wavelength $\lambda_{SPR} = 446$ nm for s and $\lambda_{SPR} = 431$ nm for p-polarized electromagnetic wave, Figure 4a. When the angle of the incidence increases, the SPR wavelength blue-shifts for both s and p polarizations of the incidence light, Figure 4c. At the angle of the incidence $\theta =$

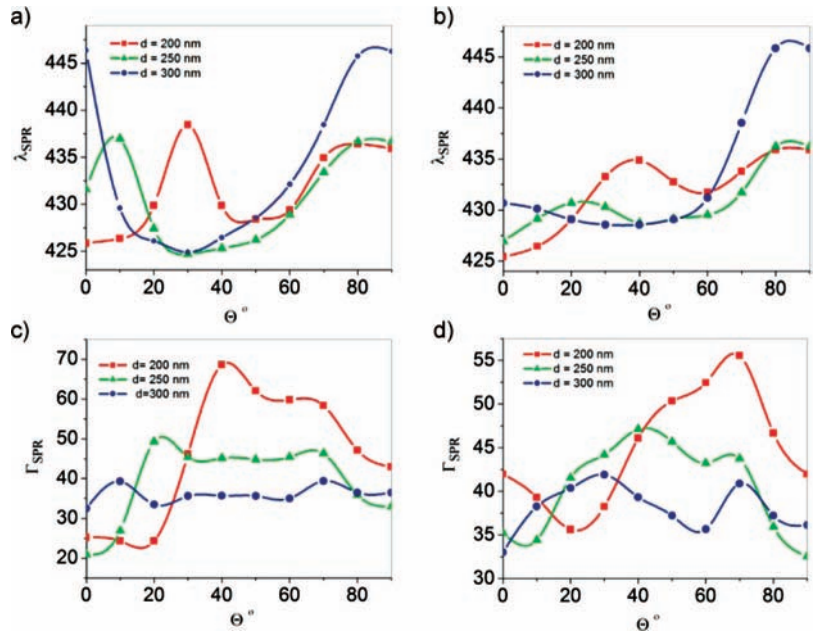

Figure 5. Dependence of the collective SPR wavelength (a, b) and bandwidth (c, d) of an array of silver spherical nanoparticles on the distance between the particles and the angle of the incidence of linear polarized electromagnetic wave: (a, c) s-polarized electromagnetic wave; (b, d) p-polarized electromagnetic wave.

30°, both s- and p-polarized SPR bands red-shift up to $\lambda_{SPR} =$ 446 nm. At the grazing angle of the incidence $\theta = 90°$ both s- and p-polarized SPR bands degenerate into single wavelength $\lambda_{SPR} =$ 445 nm. The maximum range of tuning of the SPR wavelength is $\Delta\lambda_{SPR} =$ 22 nm for s polarization and $\Delta\lambda_{SPR} =$ 18 nm for p polarization, which much larger than for both $d =$ 200 nm and $d =$ 250 nm separations. The coupling between the particles should weaken as the distance between the particle increases. In contrast, we observe a stronger coupling at a larger distance ($d =$ 300 nm) due to the resonance coupling between the particles in the chain, because the distance between the particles approaches that of the SPR wavelength of coupled mode $d \approx \lambda_{SPR}/n_{host}$,[50] where $n_{host} = 1.5$ is the index of refraction of the embedding medium. The resonant electromagnetic interaction between the particles in the chain leads to a stronger coupling between the particles, which results in a larger tuning range for the collective SPR mode. Figure 4d shows the evolution of the bandwidth of the collective SPR mode depending on the angle of the incidence of the electromagnetic mode, when the distance between the particles is $d =$ 300 nm. The maximum range of the change in the width of collective SPR resonance is $\Delta\Gamma_s =$ 10 nm and $\Delta\Gamma_p =$ 6 nm.

Figure 5 summarizes the angle dependence of the collective SPR wavelength for three distances between the particles in the chain ($d =$ 200, 250, and 300 nm). Figure 5a shows the dependence of the s-polarized electromagnetic wave as a function of the angle on the incidence. The largest range of tuning is observed for the distance $d =$ 300 nm, blue line in Figure 5a, which indicates the strongest coupling between the particles in the chain. Figure 5b shows the collective SPR wavelength for p polarization of the incident light, again, with the strongest coupling for the distance d = 300 nm between the particles in the chain. Stronger coupling between the particles in the chain "smoothes" the variation in the bandwidth on the collective SPR band when the distance between the particles approaches $d =$ 300 nm, Figure 5e,d. Increase of the distance between the particles in the chain larger than $d =$ 300 nm leads to rapid weakening of the coupling between the particles and finally to complete decoupling of the particles with the collective SPR band close to that of a single nanoparticle.

4. Conclusions

The detail numerical analysis of the scattering efficiency of a linear chain of spherical silver nanoparticles reveals a nonmonotonic dependence of the SPR wavelength and its bandwidth as a function on the angle of the incidence of the linear polarized electromagnetic wave. Far-field electromagnetic coupling between the particles in the chain leads to stronger coupling and wider range of tuning of the SPR wavelength when the distance between the particles approaches to that of the wavelength of the collective SPR in the chain. Angle resolved scattering spectra of a chain of metal nanoparticles provide an additional degree of tuning of the collective SPR in a system of electromagnetically coupled nanoparticles, which might be used, e.g., for tuning of the SPR with molecular resonances in a system of nanoparticles functionalized with target molecules. The width of the collective SPR resonance strongly depends on the coupling condition between the particles in the chain.

Acknowledgment. The author acknowledges the support from UCCS in the form of the start-up fund.

References and Notes

(1) Kreibig, U.; M., V. *Optical Properties of Metal Clusters*; Springer: Berlin, Heidelberg, 1995.
(2) Bohren, C. F.; Huffman, D. R. *Absorption and scattering of light by small particle*; Wiley: New York, 1998; Vol. xiv.
(3) Genet, C.; Ebbesen, T. *Nature* **2007**, *445*, 39.
(4) Barnes, W.; Dereux, A.; Ebbesen, T. *Nature* **2003**, *424*, 824.
(5) Park, S.; Lytton-Jean, A.; Lee, B.; Weigand, S.; Schatz, G.; Mirkin, C. *Nature* **2008**, *451*, 553.
(6) Bozhevolnyi, S.; Volkov, V.; Devaux, E.; Laluet, J.; Ebbesen, T. *Appl. Phys. A-Mater. Sci. Processing* **2007**, *89*, 225.
(7) Barnes, W.; Murray, W.; Dintinger, J.; Devaux, E.; Ebbesen, T. *Phys. Rev. Lett.* **2004**, *92*.
(8) Kelly, K.; Coronado, E.; Zhao, L.; Schatz, G. *J. Phys. Chem. B* **2003**, *107*, 668.
(9) Barhoumi, A.; Zhang, D.; Tam, F.; Halas, N. *J. Am. Chem. Soc.* **2008**, *130*, 5523.

(10) Kundu, J.; Le, F.; Nordlander, P.; Halas, N. *Chem. Phys. Lett.* **2008**, *452*, 115.
(11) Dieringer, J.; McFarland, A.; Shah, N.; Stuart, D.; Whitney, A.; Yonzon, C.; Young, M.; Zhang, X.; Van Duyne, R. *Faraday Discuss.* **2006**, *132*, 9.
(12) Laurent, G.; Felidj, N.; Grand, J.; Aubard, J.; Levi, G.; Hohenau, A.; Aussenegg, F.; Krenn, J. *Phys. Rev. B* **2006**, *73*.
(13) Ru, E.; Etchegoin, P.; Grand, J.; Felidj, N.; Aubard, J.; Levi, G.; Hohenau, A.; Krenn, J. *Curr. Appl. Phys.* **2008**, *8*, 467.
(14) Jensen, L.; Schatz, G. *J. Phys. Chem. A* **2006**, *110*, 5973.
(15) Jackson, J.; Halas, N. *Proc. Natl. Acad. Sci. U.S.A.* **2004**, *101*, 17930.
(16) Gerard, D.; Wenger, J.; Bonod, N.; Popov, E.; Rigneault, H.; Mahdavi, F.; Blair, S.; Dintinger, J.; Ebbesen, T. *Phys. Rev. B* **2008**, *77*.
(17) Yonzon, C.; Zhang, X.; Zhao, J.; Van Duyne, R. *Spectroscopy* **2007**, *22*, 42.
(18) Zhao, J.; Jensen, L.; Sung, J.; Zou, S.; Schatz, G.; Van Duyne, R. *J. Am. Chem. Soc* **2007**, *129*, 7647.
(19) Hao, E.; Li, S.; Bailey, R.; Zou, S.; Schatz, G.; Hupp, J. *J. Phys. Chem. B* **2004**, *108*, 1224.
(20) Lal, S.; Link, S.; Halas, N. *Nat. Photon.* **2007**, *1*, 641.
(21) Drezet, A.; Koller, D.; Hohenau, A.; Leitner, A.; Aussenegg, F.; Krenn, J. *Nano Lett.* **2007**, *7*, 1697.
(22) Hohenau, A.; Krenn, J.; Beermann, J.; Bozhevolnyi, S.; Rodrigo, S.; Martin-Moreno, L.; Garcia-Vidal, F. *Phys. Rev. B* **2006**, *73*.
(23) Koller, D.; Hohenau, A.; Ditlbacher, H.; Galler, N.; Aussenegg, F.; Leitner, A.; Krenn, J.; Eder, S.; Sax, S.; List, E. *Appl. Phys. Lett.* **2008**, *92*.
(24) Gobin, A.; Lee, M.; Halas, N.; James, W.; Drezek, R.; West, J. *Nano Lett.* **2007**, *7*, 1929.
(25) Krenn, J. R.; Dereux, A.; Weeber, J. C.; Bourillot, E.; Lacroute, Y.; Goudonnet, J. P.; Schider, G.; Gotschy, W.; Leitner, A.; Aussenegg, F. R.; Girard, C. *Phys. Rev. Lett.* **1999**, *82*, 2590.
(26) Holmgaard, T.; Bozhevolnyi, S. *Phys. Rev. B* **2007**, *75*.
(27) Zou, S.; Schatz, G. *J. Chem. Phys.* **2004**, *121*, 12606.
(28) Malynych, S.; Chumanov, G. *J. Opt. A-Pure Appl. Opt.* **2006**, *8*, S144.
(29) Malynych, S.; Chumanov, G. *J. Microsc.-Oxford* **2008**, *229*, 567.
(30) McMahon, M. D.; Hmelo, A. B.; Lopez, R.; Ryle, W. T.; Newton, A. T.; Haglund, R. F.; Feldman, L. C.; Weller, R. A.; Magruder, R. H. *Fabrication of ordered metallic nanocluster arrays using a focused ion beam*; Symposium on Three-Dimensional Nanoengineered Assemblies, 2002, Boston, MA; Materials Research Society: Boston, MA, December 1–5, 2002.
(31) McMahon, M.; Lopez, R.; Meyer, H. M.; Feldman, L. C.; Haglund, R. F. *Appl. Phys. B-Lasers Opt.* **2005**, *80*, 915.
(32) Moreno, E.; Garcia-Vidal, F.; Rodrigo, S.; Martin-Moreno, L.; Bozhevolnyi, S. *Opt. Lett.* **2006**, *31*, 3447.
(33) Krenn, J. R.; Weeber, J. C.; Dereux, A.; Bourillot, E.; Goudonnet, J. P.; Schider, B.; Leitner, A.; Aussenegg, F. R.; Girard, C. *Phys. Rev. B* **1999**, *60*, 5029.
(34) Tanigaki, K.; Hirosawa, I.; Ebbesen, T.; Mizuki, J.; Shimakawa, Y.; Kubo, Y.; Tsai, J.; Kuroshima, S. *Nature* **1992**, *356*, 419.
(35) Salerno, M.; Krenn, J.; Hohenau, A.; Ditlbacher, H.; Schider, G.; Leitner, A.; Aussenegg, F. *Opt. Commun.* **2005**, *248*, 543.
(36) Whitney, A.; Elam, J.; Zou, S.; Zinovev, A.; Stair, P.; Schatz, G.; Van Duyne, R. *J. Phys. Chem. B* **2005**, *109*, 20522.
(37) Hicks, E.; Zou, S.; Schatz, G.; Spears, K.; Van Duyne, R.; Gunnarsson, L.; Rindzevicius, T.; Kasemo, B.; Kall, M. *Nano Lett.* **2005**, *5*, 1065.
(38) Pinchuk, A.; Kalsin, A.; Kowalczyk, B.; Schatz, G.; Grzybowski, B. *J. Phys. Chem. C* **2007**, *111*, 11816.
(39) Sebba, D. S.; LaBean, T. H.; Lazarides, A. A. *Appl. Phys. B-Lasers Opt.* **2008**, *93*, 69.
(40) Lazarides, A. A. *Strategies for the design of plasmonically coupled nanoparticle assemblies*; 231st National Meeting of the American Chemical Society, 2006, Atlanta, GA; American Chemical Society: Washington, DC, 2006.
(41) Schatz, G.; Lazarides, A.; Kelly, K. *Abst. Pap. Am. Chem. Soc.* **2002**, *224*, U298.
(42) Haynes, C.; McFarland, A.; Zhao, L.; Van Duyne, R.; Schatz, G.; Gunnarsson, L.; Prikulis, J.; Kasemo, B.; Kall, M. *J. Phys. Chem. B* **2003**, *107*, 7337.
(43) Zou, S.; Schatz, G. *Chem. Phys. Lett.* **2005**, *403*, 62.
(44) Zou, S.; Schatz, G. *Nanotechnology* **2006**, *17*, 2813.
(45) Sung, J.; Hicks, E.; Van Duyne, R.; Spears, K. *J. Phys. Chem. C* **2007**, *111*, 10368.
(46) Chern, R. L.; Liu, X. X.; Chang, C. C. *Phys. Rev. E* **2007**, *76*.
(47) Singh, B. K.; Hillier, A. C. *Anal. Chem.* **2007**, *79*, 5124.
(48) Yonzon, C.; Jeoungf, E.; Zou, S.; Schatz, G.; Mrksich, M.; Van Duyne, R. *J. Am. Chem. Soc.* **2004**, *126*, 12669.
(49) Ghenuche, P.; Quidant, R.; Badenes, G. *Opt. Lett.* **2005**, *30*, 1882.
(50) Pinchuk, A.; Schatz, G. *Mater. Sci. Eng. B-Adv. Funct. Solid-State Mater.* **2008**, *149*, 251.
(51) Haes, A.; Zou, S.; Schatz, G.; Van Duyne, R. *J. Phys. Chem. B* **2004**, *108*, 109.
(52) Rechberger, W.; Hohenau, A.; Leitner, A.; Krenn, J.; Lamprecht, B.; Aussenegg, F. *Opt. Commun.* **2003**, *220*, 137.
(53) Fort, E.; Ricolleau, C.; Sau-Pueyo, J. *Nano Lett.* **2003**, *3*, 65.
(54) Pedersen, D. B.; Wang, S. L.; Paige, M. F.; Leontowich, A. F. G. *J. Phys. Chem. C* **2007**, *111*, 5592.
(55) Maier, S. A.; Brongersma, M. L.; Kik, P. G.; Atwater, H. A. *Phys. Rev. B* **2002**, *65*.
(56) Atay, T.; Song, J. H.; Nurmikko, A. V. *Nano Letters* **2004**, *4*, 1627.
(57) Shuford, K. L.; Ratner, M. A.; Schatz, G. C. J. Chem. Phys. 2005, *123*.
(58) Pinchuk, A.; Schatz, G. *J. Opt. Soc. Am. A-Opt. Image Sci. Vision* **2007**, *24*, A41.
(59) Pinchuk, A.; Schatz, G. *Solid-State Electron.* **2007**, *51*, 1381.
(60) Zhao, L. L.; Kelly, K. L.; Schatz, G. C. *J. Phys. Chem. B* **2003**, *107*, 7343.
(61) Mishchenko, M.; Travis, L.; Mackowski, D. *J. Quant. Spectrosc. Radiat. Transfer* **1996**, *55*, 535.
(62) Mackowski, D.; Mishchenko, M. *J. Opt. Soc. Am. A-Opt. Image Sci. Vision* **1996**, *13*, 2266.
(63) Gerardy, J. M.; Ausloos, M. *Phys. Rev. B* **1980**, *22*, 4950.
(64) Gerardy, J. M.; Ausloos, M. *Phys. Rev. B* **1982**, *25*, 4204.
(65) Mackowski, D. *J. Opt. Soc. Am. A-Opt. Image Sci. Vision* **1994**, *11*, 2851.
(66) Mackowski, D. *J. Quant. Spectrosc. Radiat Transfer* **2008**, *109*, 770.
(67) Mackowski, D. *Proc. R. Soc., London, Ser. A-Math., Phys. Eng. Sci.* **1991**, *433*, 599.
(68) Johnson, P. B.; Christy, R. W. *Phys. Rev. B* **1972**, *6*, 4370.
(69) Bouhelier, A.; Bachelot, R.; Im, J. S.; Wiederrecht, G. P.; Lerondel, G.; Kostcheev, S.; Royer, P. *J. Phys. Chem. B* **2005**, *109*, 3195.
(70) Wei, Q. H.; Su, K. H.; Durant, S.; Zhang, X. *Nano Lett.* **2004**, *4*, 1067.
(71) Corrigan, T. D.; Guo, S. H.; Szmacinski, H.; Phaneuf, R. J. *Appl. Phys. Lett.* **2006**, *88*.
(72) Meier, M.; Wokaun, A.; Liao, P. F. *J. Opt. Soc. Am. B-Opt. Phys.* **1985**, *2*, 931.
(73) Carron, K. T.; Fluhr, W.; Meier, M.; Wokaun, A.; Lehmann, H. W. *J. Opt. Soc. Am. B-Opt. Phys.* **1986**, *3*, 430.
(74) Salerno, M.; Krenn, J. R.; Hohenau, A.; Ditlbacher, H.; Schider, G.; Leitner, A.; Aussenegg, F. R. *Opt. Commun.* **2005**, *248*, 543.
(75) Lamprecht, B.; Schider, G.; Lechner, R. T.; Ditlbacher, H.; Krenn, J. R.; Leitner, A.; Aussenegg, F. R. *Phys. Rev. Lett.* **2000**, *84*, 4721.
(76) Haynes, C. L.; McFarland, A. D.; Zhao, L. L.; Van Duyne, R. P.; Schatz, G. C.; Gunnarsson, L.; Prikulis, J.; Kasemo, B.; Kall, M. *J. Phys. Chem. B* **2003**, *107*, 7337.
(77) Zhao, L.; Kelly, K.; Schatz, G. *J. Phys. Chem. B* **2003**, *107*, 7343.
(78) Rechberger, W.; Hohenau, A.; Leitner, A.; Krenn, J. R.; Lamprecht, B.; Aussenegg, F. R. *Opt. Commun.* **2003**, *220*, 137.
(79) Pinchuk, A. O.; Schatz, G. C. *Nanoparticle optical properties: Far- and near-field electrodynamic coupling in a chain of silver spherical nanoparticles*; Symposium on Sub-wavelength Photonics Throughout the Spectrum held at the E-MRS 2007 Spring Conference, 2008, Strasbourg, France.

JP811067R